Research Article

Journal of Applied Material Science & Engineering Research

Optical Absorption and Photoluminescence in the Spherical *InP*/InSb/*InP* Core/shell/ shell Nano Structure

Harutyunyan VA[1], Kazaryan EM[1] and Hayrapetyan DB[1,2]

[1]*Russian-ArmenianUniversity, H. Emin123, 0051, Yerevan, Armenia*

[2]*Peter The Great Saint, Peters burg Polytechnical University, Polytechnic heskaya29, St. Petersburg, 195251, Russia*

***Corresponding author**

Hayrapetyan DB, Russian-Armenian University, 123 HovsepEmin Str., Yerevan 0051, Armenia, E-mail: dhayrap82@gmail.com

Submitted: 05 Apr 2018; **Accepted**: 13 Apr 2018; **Published**: 30 Apr 2018

Abstract

The one particle states of charge carriers are considered in InP/InSb/InPcore/shell/shell spherical quantum nano structure at the regime of strong quantization. The results of numerical calculations for the values of the energy of charge carriers for different values of the thickness of the quantizing layer of InSb are presented. The calculations were performed with allowance for the Kaned is persion for electrons and light holes in the InSb layer. The dependence of the number and position of the energy levels of charge carriers in the quantizing layer of InSb on the width of the well (layer thickness) is shown. The dependence of the absorption coefficient and photoluminescence spectra on the energy of incident light of interband transitions have been investigated. The oscillator strengths and selection rules for these transitions have been obtained. The absorption has a strictly resonant character. By the orbital and azimuthal numbers only diagonal inter band transitions are possible. For the radial number, the transitions between the states with the same radial numbers have the highest intensity.

Keywords: Core/shell/shell, Spherical Quantum Layer, Size Quantization, Optical Absorption, Photoluminescence

Introduction

Indium antimonide (InSb) is the only semi conductor material, which can be used for three types of photo detectors: photo conductive (photo resistance), photo voltaic and photo electro-magnetic. It is one of the main materials for photo detectors, which operates in the range of 3-5 m. The unique properties of *InSb* make possible also to use it in the broadband of civil applications including medicine and ecological monitoring [1]. The optical properties of *InSb* have, of course, been long studied and are well understood [2]. There is no doubt that the presence of unique features, such as narrow band gap, high carrier mobility etc. [3], the size quantization fact or opens new opportunities for the device application of *InSb*. Hence, *InSb* remains significantly interesting material for the fundamental investigation of its nanostructure for potential application, such as kind nano electronic devices [3]. Nowadays quantum wells (films) [4], quantum wires [3,5] and quantum dots [6] on the basis of *InSb* have wide range of applications. At the same time, in the last two decades spherically symmetrical semi conductor hetero phase core/shell/shell structures [7-12] are also intensively studied. This is due to the fact that the increasing application of nano materials requires the development of new materials and structures. The requirements dictate that these materials and structures be capable of performing several tasks and functions within the frame work of the unified nanometric geometry [13-17]. In particularly, spherically symmetrical core/shell/shell structures simultaneously combine and synthesize in itself a number of properties of both quantum dots and quantum films. In the point of view of device application they are more multi-functional than the separate single quantum films and quantum dots [18,19]. In this regard, one of the technically realizable and promising for the application of core/shell/shell structures based on *InSb* is spherically symmetrical composition of *InP/InSb/InP* [20]. Let us note that in several works the electronic and optical effects are considered via various approximations in single spherical nano layer of *InSb* [21-23]. However, the consideration and quantitative description of electronic states and optical transitions have not performed yet in *InSb* nano layer, which is a component of real hetero phase *InP/InSb/InP* structure.

In the present work, the calculations of charge carrier's energetic spectrum in the *InSb* nano layer of *InP/InSb/InP* spherical hetero composition are presented, as well as the results of theoretical investigation of optical absorption and photoluminescence in such layer are shown.

One-Particle States in *Insb* Nano layer of Spherical Hetero Composition *Inp/Insb/Inp*

Before presenting one-particle state calculations, let us present the basic physical characteristics of bulk crystals *InP* and *InSb*.

Table1: The basic physical characteristics of bulk crystals InP and *InSb* [24-28]

Mate-rial	Latticeconstant a_0(nm)	Bandgap E_g (eV)	Excitonradius a_{ex}(nm)	Electronaffinity U_c(eV)	Electroneff. mass μ_e/m_0	Heavyholeeff. mass $s\mu_{hh}$	Lightholeeff. mass $\mu lh / m_0$
InP	0.58687	1.344	10 15	-4.38	0.08	0.6	0.089
InSb	0.6479	0.17	65	-4.59	0.0145	0.43 0.6	0.015

Here m_0 is the mass of free electron. As it can be seen from the Table1, the band off sets of energy on the interface of contacting materials areΔU_c =0.21 eV and ΔU_v =0.964 eV for the conduction and valence bands, respectively. For instance, in this case the *InSb* nanolayer of the composition *InP/InSb/InP* is presented as a potential well with ΔU_c =0.21 eV and ΔU_v =0.964 eV depths for electron in conductor band and for hole states in valence band, respectively.

Before proceeding to the specific calculations, let us adjust corresponding designations and the values of the parameters, which will be used in following numerical calculations.

For *Inp:* $a_{ex} \equiv a_1 = 12$nm; $\mu_e \equiv \mu_{e,1} = 0.08\ m_0$; $\mu_{lh} \equiv \mu_{lh,1} = 0{,}1\ m_0$; $\mu_{hh,1} = 0{,}6m_0$.
For *Inp:* $a_{ex} \equiv a_2 = 60$nm; $\mu_e \equiv \mu_{e,2} = 0.0145\ m_0$; $\mu_{lh} \equiv \mu_{lh,1} = 0{,}0145\ m_0$; $\mu_{hh,2} = 0{,}5m_0$.

In this problem a_1= 12 nm will be as a length unit, and

$E_{unit} = \frac{\hbar^2}{2\mu_{e,1}a_1^2} = 3{,}315 \cdot 10^{-3}$ eV as an energy unit.

Let's denote the inner and outer radii of the *InSb* layer by R_1 and R_2 , respectively, and *L=R2 - R1* is the thickness of the layer. In the calculations, the layer's thickness varies in the range of nm. It is clearly seen from the Table1 that in the *InSb* layer the Coulomb interaction between the electron and hole can be neglected for such valuesof the layer's thickness. That is, in the case under consideration the strong size quantization regime will be realized with sufficient accuracy for the charge carriers in the *InSb* layer. The value of the layer thickness *L=24* nm is, in fact, the maximum permissible, when a strong quantization regime realizes in *InSb* layer. All calculations are made in the effective mass approximation.

Let us *InSb* layer approximate by rectangular potential well with finite depth in the radial direction. It can be written for the potential energy of the particle:

$$V(r) = \begin{cases} \Delta U_{c,v}; & 0 \le r \le R_1, r \ge R_2, \\ 0; & R_1 \le r \le R_2. \end{cases} \quad (1)$$

In this model, we now consider the single-particle states of charge carriers in *InSb* layer.

As it is known, in *InSb* Kane dispersion law occurs for electrons (also for light holes), which has the following for min the two-band model [29,30]:

$$E_e = \sqrt{\vec{p}_e^2 s^2 + \mu_{e,2}^2 s^4};\ s \sim 10^6\, m/sec \quad (2)$$

Here $\vec{p}$ is the full momentum of the particle. In the core and outer layer (*InP*) carrier dispersion law will be assumed strongly quadratic.

In spherical coordinates (r, ϑ, φ), the total wave function of the particle ψ (r, ϑ, φ) will be found in the following form:

$$\Psi(r,\vartheta,\varphi) = \Phi(r)Y_{l,m}(\vartheta,\varphi) = \frac{\chi(r)}{\sqrt{r}}Y_{l,m}(\vartheta,\varphi) \quad (3)$$

Here $Y_{l,m}(\vartheta, \varphi)$ are the normalized spherical functions, and l =0,1,2...., m=0, ± 1,2,... are the orbital and azimuthal quantum numbers, respectively [31].

We obtain the following equations for radial wave functions in region1 (core *InP*), region2 (first shell, *InSb* layer) and region3 (second shell, *InP*), respectively:

$$\rho^2\frac{d^2\chi_1(\rho)}{d\rho^2} + \rho\frac{d\chi_1(\rho)}{d\rho} - \left[k_1^2\rho^2 + \left(l+\frac{1}{2}\right)^2\right]\chi_1(\rho) = 0, \quad (3)$$

$$\rho^2\frac{d^2\chi_2(\rho)}{d\rho^2} + \rho\frac{d\chi_2(\rho)}{d\rho} + \left[k_2^2\rho^2 - \left(l+\frac{1}{2}\right)^2\right]\chi_2(\rho) = 0, \quad (4)$$

$$\rho^2\frac{d^2\chi_3(\rho)}{d\rho^2} + \rho\frac{d\chi_3(\rho)}{d\rho} - \left[k_3^2\rho^2 + \left(l+\frac{1}{2}\right)^2\right]\chi_3(\rho) = 0. \quad (5)$$

Here $\rho = \frac{r}{a_1}$ $k_1^2 = \Delta U_c / E_{unit} - \varepsilon_e$ $k_2^2 = \frac{E_{unit}\varepsilon_e^2}{2\mu_{e,1}s^2} - \frac{\mu_{e,2}^2 s^4}{2\mu_{e,1}s^2 E_{unit}}$ $k_3^2 = k_1^2$, $\varepsilon_e = E_e / E_{unit}$ and E_e -is the full energy of the electron in *InSb* layer. The solutions of these equations satisfying finiteness conditions when r→0 and vanishing, when r→∞ , are given by the following expressions [32]:

$$\chi_1(\rho) = AI_{l+1/2}(k_1\rho), \quad (6)$$

$$\chi_2(\rho) = B_1 J_{l+1/2}(k_2\rho) + B_2 J_{-(l+1/2)}(k_2\rho), \quad (7)$$

$$\chi_3(k_3\rho) = CK_{l+1/2}(k_3\rho). \quad (8)$$

Here $J_v(x)$ is the first order Bessel function, and $I_v(x)$ and $K_v(x)$ -modified Bessel functions of the first and second kind (Infield and Macdonald functions), respectively, and A, B_1,B_2 C are the normalization constants. We obtain the following condition after a cross-linking of the logarithmic derivatives of functions (7)-(9) on the borders of the well (r = R1 and r = R_2) for determining the energy spectrum of electrons in the *InSb* layer:

$$\frac{(a\rho_1)J'_{-(l+1/2)}(a\rho_1) - (b\rho_1)J_{-(l+1/2)}(a\rho_1)\dfrac{I'_{l+1/2}(b\rho_1)}{I_{l+1/2}(b\rho_1)}}{(a\rho_1)J'_{l+1/2}(a\rho_1) - (b\rho_1)J_{l+1/2}(a\rho_1)\dfrac{I'_{l+1/2}(b\rho_1)}{I_{l+1/2}(b\rho_1)}} = \frac{(a\rho_2)J'_{l+1/2}(a\rho_2) - (b\rho_2)J_{l+1/2}(a\rho_2)\dfrac{K'_{l+1/2}(b\rho_2)}{K_{l+1/2}(b\rho_2)}}{(a\rho_2)J'_{-(l+1/2)}(a\rho_2) - (b\rho_2)J_{-(l+1/2)}(a\rho_2)\dfrac{K'_{l+1/2}(b\rho_2)}{K_{l+1/2}(b\rho_2)}}. \quad (9)$$

In the case of electrons for the parameters *a* and b the following expressions were obtained:

$$a = k_{e,2} = \sqrt{0,00364\varepsilon_e^2 - 2,255}\ ,\ b = k_{e,1} = \sqrt{63,35 - \varepsilon_e}\ .$$

Derivative Bessel functions are calculated by the full argument.

The size quantization effect, as it is known, is mostly pronounced for the lower energy states of the charge carriers. Accordingly, we are interested in the several first solutions of the equation (10), which correspond to small valuesof quantum numbers. Consider the case of a relatively thin layer for visual clarity, when the number of states in the quantum well is not large.

In the Table2 presented solutions of equation (10) illustrate the dependence of the electron energy levels and their position in the *InSb* quantum well when changing the layer thickness in the range of $L \leq 15$ nm. The calculations are made for the fixed value of the core radius R_1=12 nm (p_1=1) and the depth of the well ΔU_c=0.21 eV.

Table 2: Variation of the number of electronic energy levels in the *InSb* quantum well layer by changing the layer thickness in the range of L ≤ 15 nm.

Layer'sthickness *L* (nm)	Numbero flevels	levels	Energy $E_{n,l}$ (meV)
L = 2.33	1	n=1, l=0;	$E_{1.0}$ = 105.38
L = 3.29	2	n=1, l=0; n=1, l=1;	$E_{1.0}$ = 100.21 $E_{1.1}$ = 105.68
L = 4.57	3	n=1, l=0; n=2, l=0; n=1, l=1;	$E_{1.0}$ = 99.98 $E_{2.0}$ = 197.77 $E_{1.1}$ = 181.36
L = 11.06	4	n=1, l=0; n=2, l=0; n=1, l=1; n=1, l=2;	$E_{1.0}$ = 91.20 $E_{2.0}$ = 152.09 $E_{1.1}$ = 138.93 $E_{1.2}$ = 163.76
L = 13.43	5	n=1, l=0; n=2, l=0; n=1, l=1; n=2, l=1; n=1, l=2;	$E_{1.0}$ = 89.11 $E_{2.0}$ = 141.82 $E_{1.1}$ = 130.98 $E_{2.1}$ = 201.55 $E_{1.2}$ = 150.17
L = 15.36	6	n=1, l=0; n=2, l=0; n=3, l=0; n=1, l=1; n=2, l=1; n=1, l=2;	$E_{1.0}$ = 87.88 $E_{2.0}$ = 135.08 $E_{3.0}$ = 198.57 $E_{1.1}$ = 125.47 $E_{2.1}$ = 188.49 $E_{1.2}$ = 146.06

As it is already noted, the dispersion law of light holes is also described by the expression (2) and, respectively, the energy levels of the light holes will also be determined from the expression of the form (10). The depth of the potential well for the hole states (ΔU_v= 0.964 eV) is much greater than the depth of the well of the electronic states (ΔU_v= 0.21 eV). Accordingly, the number of quantum levels for hole states (in the case of both light and heavy holes) at the same layer thickness of the quantum well in the valence band is considerably more than the number of levels of electronic states. We will not give here for the hole state table similar to Table 2, and note only that the energy of hole states at the same layer thickness ($L \leq 15$ nm) when l=0 changes in the intervals of $E_{lh} \in$[191.33meV] and $E_{hh} \in$[1.01me - V.36meV] for the cases of light and heavy holes, respectively.

Optical Absorption and Photoluminescence in *Inp/Insb/Inp* Nano Structure

Let us consider the inter band optical transitions in this core/shell/shell nano structure, when *L=24* nm. As noted above, it is the maximum range of thickness values when in *InSb* layer the excit on effect can be neglected with sufficient accuracy.

Consider the dimension less oscillator strength, which is defined in the following way [33]:

$$J = f_{v_e,v_h} / f_0 = \int \Psi_e\left(\vec{r}_e\right)\Psi_h\left(\vec{r}_h\right)dV \qquad (10)$$

Where f_0 is the oscillator strength of the bulk material, $Ve = \{n_e, l_e, m_e\}$ and $Ve = \{n_h, l_h, m_h\}$ are the sets of quantum numbers of the electron and light/or heavy hole, respectively. The values of the oscillator strength for the transitions from heavy and light hole states to the electron states are presented in the Table3.

Table 3: Values of the oscillator strength for $|v_{lh}\rangle \rightarrow |c_e\rangle$ and $|v_{lh}\rangle \rightarrow |c_e\rangle$ inter band optical transitions, when R_1=12 nm, R_2=36 nm.

$n_{lh,hh}, l_{lh,hh}\rangle \rightarrow |n_e, l_e\rangle$	$f_{lh\rightarrow e}/f_0$	$f_{hh\rightarrow e}/f_0$
Diagonal Transitions		
$\|1,0\rangle \rightarrow \|1,0\rangle$	0.9987	0,9998
$\|2,0\rangle \rightarrow \|2,0\rangle$	0.9736	0.9824
$\|3,0\rangle \rightarrow \|3,0\rangle$	0.9687	0,9601
$\|1,1\rangle \rightarrow \|1,1\rangle$	0.9955	0,9975
$\|1,2\rangle \rightarrow \|1,2\rangle$	0.9886	0,9973
$\|2,1\rangle \rightarrow \|2,1\rangle$	0.9754	0,9932
$\|2,2\rangle \rightarrow \|2,2\rangle$	0.9691	0.9816
Non-diagonal Transitions		
$\|2,0\rangle \rightarrow \|1,0\rangle$	0.2417	0,1249
$\|3,0\rangle \rightarrow \|1,0\rangle$	0.1325	0,0291
$\|1,1\rangle \rightarrow \|2,1\rangle$	0.1284	0,1425
$\|1,1\rangle \rightarrow \|3,1\rangle$	0.0381	0,0525
$\|2,1\rangle \rightarrow \|1,1\rangle$	0.0067	0.0139
$\|2,2\rangle \rightarrow \|1,2\rangle$	0.0044	0.0048
$\|3,1\rangle \rightarrow \|1,1\rangle$	0.0018	0.0087

The presence in Exp.(3) of spherical functions $Y_{lm}(\vartheta, \varphi)$ leads by orbital and azimuthal quantum numbers to the selection rules l_e-l_h=0 and $|m_e|$-$m_h|$=0, respectively.

Regarding the selection rules for the radial number n, in Table3 data demonstrate the following: transitions diagonally by radial number have the greatest intensity, and non-diagonal transitions are strongly suppressed ($f_{eh}/f_0 \ll 1$). The intensity of the diagonal transition slowly decreases with increasing the values of both radial and orbital quantum numbers. The intensity of off-diagonal transitions decreases with increasing the degree of off-diagonality. So from a practical point of view, in the considered system inter band optical diagonal transitions by the radial number have a real interest. The threshold frequency of these transitions is determined by the relation

$$\hbar\omega_{e,h} = E_g^L + E_e + E_h \qquad (11)$$

$$\Delta_g = \hbar\omega_{e,h} - E_g^L \qquad (12)$$

Here E^L_g –is the band gap width of the bulk *InSb* sample, and *e,h* a reset of quantum numbers of the electron and hole states, respectively, ω is frequency of the incident light. The main contribution in the band gap effective broadening

Makes the radial quantized motion of the charge carriers. For a fixed value of the radial number, the variation of the band gap will be determined by the orbital number of charge carrier $l_e = l_h$. Table4 shows the values of the effective broadening band gap of *InSb* layer for different inter band transitions.

Table 4: Effective broadening band gap of *InSb* layer with different inter band transitions, when R_1=12 nm, R_2=36 nm.

Transitions	$\|2,1\rangle \rightarrow \|1,1\rangle$	$\|2,1\rangle \rightarrow \|1,1\rangle$	$\|2,1\rangle \rightarrow \|1,1\rangle$	$\|2,1\rangle \rightarrow \|1,1\rangle$	$\|2,1\rangle \rightarrow \|1,1\rangle$	$\|2,1\rangle \rightarrow \|1,1\rangle$
Δ_g^{lh}(eV)	0.2497	0.3144	0.3793	0.3847	0.4871	0.5598
Δ_g^{hh}(eV)	0.0962	0.1107	0.1265	0.1383	0.1541	0.1746

Now let us consider the inter band optical absorption in the real ensemble of core/shell/shell nano structures with the dispersion of their sizes in the regime of strong size quantization. Note that this dispersion will lead to broadenings of spectral lines.

According to [34] we have following expression for light absorption coefficient for the strong quantization regime:

$$K(\omega) = K_0 \sum_{\nu_e,\nu_h} J^2 \delta\left(\hbar\omega_{e,h} - E_g^L - E_e - E_h\right) \qquad (13)$$

Where E_g is the energy gap of the semiconductor, K_0 -is a quantity proportional to the square of modulus of the matrix element of the dipole moment taken over the Bloch functions. The broadenings of spectral lines will be taken into account with the help of replacing the delta function in expression (13) by Lorentz contour:

$$\delta\left(\hbar\omega_{e,h} - E_g^L - E_e - E_h\right) \rightarrow \frac{\Gamma}{\left(\left(\hbar\omega_{e,h} - E_g^L - E_e - E_h\right)^2 + \Gamma^2\right)} \qquad (14)$$

Where Γ -the width of Lorentzian parameter. For calculations we take Γ=5*meV* according to [35].

The next step of the investigation of the *InP/InSb/InP* Core/Shell/Shell structure's optical properties is the calculation of the photoluminescence (PL) spectra. The photoluminescence spectra is calculated using the Roosbroeck-Shockley relation [36,37]:

$$R(\hbar\omega) = R_0 \hbar\omega K(\hbar\omega) \frac{f_c(1-f_v)}{f_v - f_c} \qquad (15)$$

where R_0 is proportional to the square of modulus of the matrix element of the dipole moment taken over the Bloch functions, f_c and 1 - f_v are probabilities of the conduction band states being occupied and the valance band states being empty, respectively. For the high temperatures the term $\frac{f_c(1-f_v)}{f_v - f_c}$ in Roosbroeck-Shockley relation transforms into the Boltzmann like form.

Discussion of Results

Let us now consider the results obtained with reference to optical inter band transitions in the structure under study. The results presented in Table3 clearly show that the quantum size effect in this structure is especially pronounced in the *InSb* nano layer of the general structure of the core/shell/shell. Indeed, for transitions between states with identical radial numbers (Fig.1, Fig.3), the absorption has an essentially resonant character. Ideally (in the model of an infinitely deep well for the *InSb* layer), these peaks become delta-shaped needles of equal height. The intensity of transitions between states with unequal radial numbers is less, the greater the degree of non-diagonality of the transitions (Fig.2, Fig.4). In the same ideal, these curves simply disappear. Those, the results of the calculations show that the proposed model physically adequately describes the system under consideration and that in this hetero structure charge carrier' localization due to size quantization occurs precisely in the *InSb* nano layer.

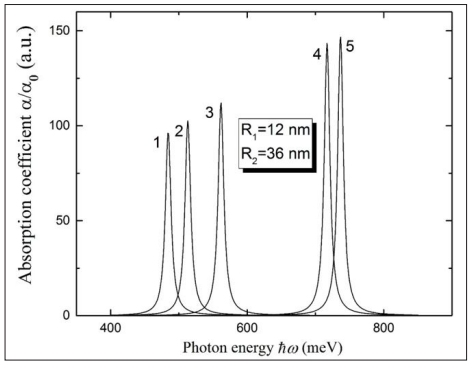

Figure 1: The dependence of the absorption curve for the diagonal transitions between light-hole and electron on the frequency of the incident light:1) $|1,0\rangle \rightarrow |1,0\rangle$, 2) $|1,0\rangle \rightarrow |1,0\rangle$, 3) $|1,0\rangle \rightarrow |1,0\rangle$, 4) $|1,0\rangle \rightarrow |1,0\rangle$,5)$|1,0\rangle \rightarrow |1,0\rangle$.

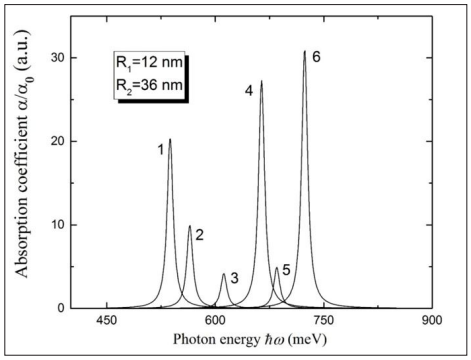

Figure 2: The dependence of the absorption curve for the off-diagonal transitions between light-hole and electron on the frequency of the incident light: 1) $|2,0\rangle \rightarrow |1,0\rangle$, 2) $|2,1\rangle \rightarrow |1,1\rangle$, 3) $|1,0\rangle \rightarrow |2,0\rangle$,4) $|1,1\rangle \rightarrow |2,1\rangle$,5)$|2,2\rangle \rightarrow |2,1\rangle$,6)$|2,1\rangle \rightarrow |2,2\rangle$.

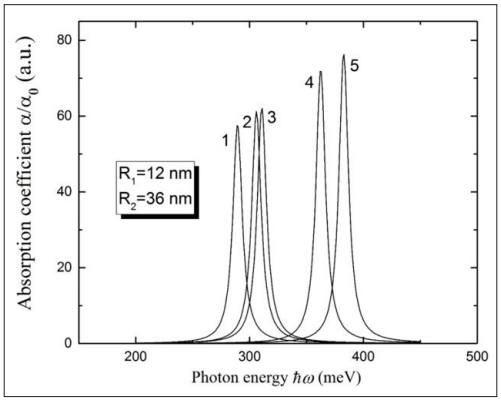

Figure 3: The dependence of the absorption curve for the diagonal transitions between heavy-hole and electron on the frequency of the incident light: 1) $|1,0\rangle\rightarrow|1,0\rangle$, 2) $|1,1\rangle\rightarrow|1,1\rangle$, 3) $|1,2\rangle\rightarrow|1,2\rangle$, 4) $|2,0\rangle\rightarrow|2,0\rangle$, 5) $|2,1\rangle\rightarrow|2,1\rangle$

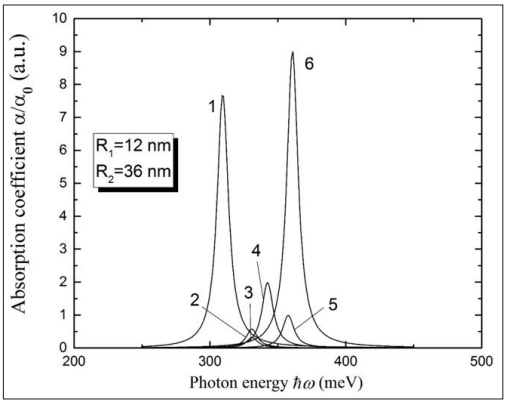

Figure 4: The dependence of the absorption curve for the off-diagonal transitions between heavy hole and electron on the frequency of the incident light: 1) $|2,0\rangle\rightarrow|1,0\rangle$, 2) $|2,1\rangle\rightarrow|1,1\rangle$, 3) $|1,0\rangle\rightarrow|2,0\rangle$, 4) $|1,1\rangle\rightarrow|2,1\rangle$, 5) $|2,2\rangle\rightarrow|2,1\rangle$, 6) $|2,1\rangle\rightarrow|2,2\rangle$

The Fig.1 and Fig.2 show the dependence of the absorption coefficient for the diagonal and off-diagonal inter band optical transitions, correspondingly, between light-hole and electron on the frequency of the incident light. The sets of the peaks correspond to the different quantum transitions. As the oscillator strengths for the diagonal transitions with a high accuracy are equal to one therefore the intensity values are the same for the all diagonal transitions. The opposite situation is observed for the off-diagonal transitions.

The Fig.3 and Fig.4 show the dependence of the absorption coefficient for the diagonal and off-diagonal inter band optical transitions, correspondingly, between heavy-hole and electron on the frequency of the incident light.

Note that the PL curveshave been calculated for the room temperature. The separate peaks corresponding to the transitions described in the absorption part can be seen in the PL spectra. As we mention above for the high temperatures the term $\frac{f_c(1-f_v)}{f_v-f_c}$ in Roosbroeck-Shockley relation transforms into the Boltzmann like form and this term vanishes the peaks in the high-energy region. That is why the low energy peaks can be observed more clearly in the PL spectra than the high-energy peaks [38,39]. It is also obvious that the peaks corresponding to the diagonal transitions have higher intensity than the peaks corresponding to the non-diagonal transitions.

The dependence of the PL intensity on the frequency of the incident light for the heavy-hole electron diagonal and non-diagonal transitions are shown in Fig. 5 and Fig. 6, respectively. As we can see from the PL spectra for light hole - electron and heavyhole - electron transitions the intensity of the PL spectra increases with the increase of temperature. The same dependences of the PL spectra for the light-hole electron diagonal and non-diagonal transitions are shown in Fig. 7 and Fig. 8, respectively. Note that the intensity PL spectra increaseswith the increase of the temperature, while in experiments the opposite behaviour is observed. This is due to the fact that we have not considered the interaction of the exciton with phonons, the amount of which increases with the increase of temperature. In this case, the non-radiative recombination processes increases and the intensity of the PL spectra decreases.

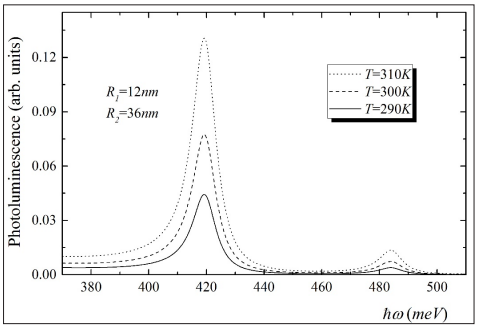

Figure 5: The dependence of the photoluminescence intensity for light hole - electron diagonal transitions on the frequency of the incident light in arbitrary units.

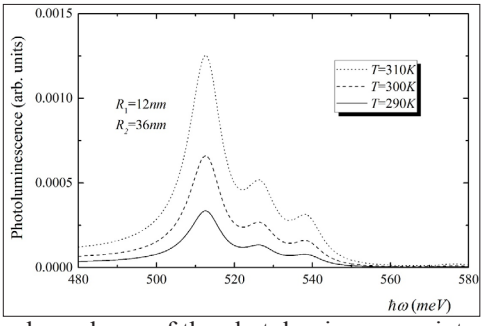

Figure 6: The dependence of the photoluminescence intensity for light hole - electron non-diagonal transitions on the frequency of the incident light in arbitrary units.

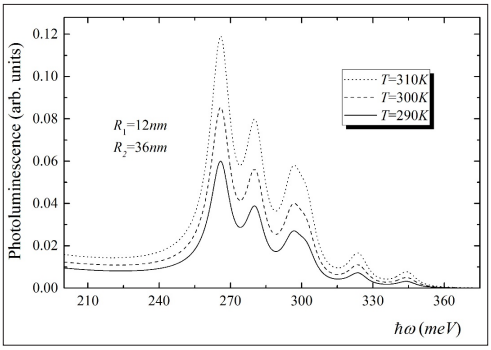

Figure 7: The dependence of the photoluminescence intensity for heavy hole - electron diagonal transitions on the frequency of the incident light in arbitrary units.

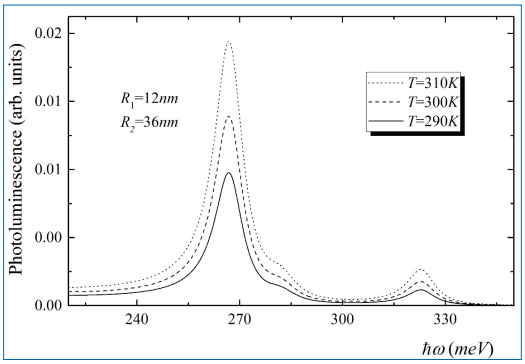

Figure 8: The dependence of the photoluminescence intensity for heavy hole - electron off-diagonal transitions on the frequency of the incident light in arbitrary units.

Conclusion

Concerning the results obtained in the work, we can conclude the following:

- The model proposed in the paper physically adequately describes the states of charge carriers in the spherical hetero phase core/shell/shell structure of *InP/InSb/InP* in the strong-quantization regime.
- In the wide range of changes in the thickness of the *InSb* layer, in the layer the carrier states are described with sufficient accuracy by single-particle wave functions without taking into account the Coulomb interaction between the electron and the hole.
- In the same range, the thickness of the layer can be controlled in the controlled manner by the width of the band gap of the *InSb* layer, ie, it is possible to control the frequency of absorption- transmission of the incident light wave in a controlled manner.
- Along with the thickness of the layer, an important factor is also the large difference between the values of the effective masses of electrons and heavy holes in the frequency spectrum of inter band absorption. In this structure, this factor is one of the most important again due to the localization of charge carriers in the *InSb* layer.

Acknowledgment

This work was supported by the RAMES State Committee of Science, in the frames of their search project t.№16YR-1C022.

References

1. A Vaseashta, S Khudaverdyan (2013) Advanced Sensors of Safety and Security, Springer 375.
2. Springer Handbook of Crystal Growth, Springer Science & Business Media (2010) 346-352.
3. Kuo CH, Wu JM, Lin SJ (2013) Room temperature-synthesized vertically aligned *InSb* nano wires: electrical transport and field emission characteristics. Nano scale Res Lett 8: 69-72.
4. *InSb* quantum well structures for electronic device applications, by Ediriso oriya Madhavie, The University of Oklahoma (2009) 159 pages; Fabrication and Characterization of an *InSb* Quantum Well Device, Marina Hesselberg, Kopenhagen University (2013) 29.
5. Shafa M, Akbar S, Gao L, Fakhar-E-Alam M, Wang ZM (2016) Indium Antimonide Nano wires: Synthesis and Properties. Nano scale Res Lett 11: 164-167.
6. Wang T, Vaxenburg R, Liu W, Rupich SM, Lifshitz E (2015) Size-Dependent Energy Levels of *InSb* Quantum Dots Measured by Scanning Tunneling Spectroscopy. ACS Nano 9: 725-732.
7. Reiss P, Protie`re M, Li L (2009) Core/Shell Semi conductor Nano crystals Wiley-VCH Verlag GmbH & Co. K Ga A, Weinheim, www.small-journal.com, small No.2 154-168.
8. Ferron A, Serra P, Osenda O (2012) Near-threshold properties of the electronic density of layered quantum dots Phys Rev B85 165322-1-6.
9. M´elinon P, Begin-Colin S, Duvail JL, Gauffre F, Boime NH, et al. (2014) Engineered /shell nano particles. Physics Reports Elsevier 543: 163-197.
10. Hayrapetyan DB, Kazaryan EM, Petrosyan LS, Sarkisyan HA (2015) Core/shell/shell spherical quantum dot with Kratzer confining potential: Impurity states and electrostatic multipoles. Physica E: Low-dimensional Systems and Nanostructures 66: 7-12.
11. Hayrapetyan DB, Amirkhanyan SM, Kazaryan EM, HA Sarkisyan EM (2016) Effect of hydrostatic pressure on diamagnetic susceptibility of hydrogenic donor impurity in core/shell/shell spherical quantum dot with Kratzer confining potential. Physica E: Low-dimensional Systems and Nanostructures 84: 367-371.
12. Harutyunyan VA, Hayrapetyan DB, Baghdasaryan DA (2016) Single-electron states in semiconductor nanospherical layer of large radius. Journal of Contemporary Physics 51: 350-359.
13. Chaudhuri RG, Paria S (2012) Core/Shell Nano particles: Classes, Properties, Synthesis Mechanisms, Characterization, and Applications. Chem Rev 112: 2373-2433.
14. M´elinon P, Begin-Colin S, Duvail JL, Gauffre F, Boime NH, et al. (2014) Engineered inorganic core/shell nano particles. Physics Reports Elsevier 543: 163-197.
15. Holovatsky VA, Bernik IB (2014) Effect of magnetic and electric fields on optical properties of semi conductor spherical layer, Semi conductor Physics. Quantum Electronics & Opto electronics 17: 7-13.
16. MohamedEl-Toni A, Habila MA, Labis JP, ALOthman ZA, Alhoshan M, et al. (2016) Design, synthesis and applications of core–shell, hollow core, and nano rattle multi functional nano structures. Nano scale 8: 2510-2531.
17. Baghdasaryan DA, Hayrapetyan DB, Harutyunyan VA (2017) Optical transitions in semiconductor nano spherical core/shell/shell hetero structure in the presence of radial electro static field. Physica B 510: 33-37.
18. Henini (2011) Handbook of Self Assembled Semiconductor Nano structures for Novel Devices in Photonics and Electronics Elsevier 864.
19. Chaudhuri RGh, Paria S (2012) Core/Shell Nano particles: Classes, Properties, Synthesis Mechanisms, Characterization, and Applications, Chem Rev 112: 2373-2433.
20. Zoheir M, Manaselyan AKh, Sarkisyan HA (2008) Electronic states and the Stark shift in narrow band *InSb* quantum spherical layer. Physica E: Low-dimensional Systems and Nano structures 40: 2945-2949.
21. Kazaryan EM, Kirakosyan AA, Mughnetsyan VN, Sarkisyan HA (2012) Tunability of absorption threshold frequencies and Stark shift in the *InSb* narrow gap spherical quantum layer". Semiconductor Science and Technology 27: 6.
22. Amirkhanyan SM, Kazaryan EM, Sarkisyan HA (2015) Calculation of electro static multi poles of electron localized

in narrow-band *InSb* spherical nano layer". Journal of Contemporary Physics 50: 268-276.
23. http://www.ioffe.ru/SVA/NSM/Semicond/InP/basic.html http://www.ioffe.ru/SVA/NSM/Semicond/InP/bandstr.html http://www.ioffe.ru/SVA/NSM/Semicond/*InSb*/basic.html http://www.ioffe.ru/SVA/NSM/Semicond/*InSb*/bandstr.html
24. Sneha G Pandya, MartinEKordesch (2015) Characterization of *InSb* Nano particles Synthesized Using Inert Gas Condensation. Nano scale Res Lett 10: 258-261.
25. Wang Y, Yang X, He TC, Gao Y, Demir HV (2013) Near resonant and non resonant third-order optical non linearities of colloidal InP/Zn Squantum dots. Appl Phys Lett 102: 021917-1-4.
26. Mushonga P, Onani MO, Madiehe AM, Meyer M (2012) Indium Phosphide- Based Semiconductor Nano crystals and Their Applications Hindawi Publishing Corporation Journal of Nano materials 11.
27. Buhro WE, Colvin VL (2003) Semiconductor nano crystals: Shape matters, Nature Materials 2,138-139; Tamang S, Lincheneau C, Hermans Y, Jeong S, Reiss P (2016) Chemistry of InP Nano crystal Syntheses. Chem Mater 28: 2491-2506.
28. Reece JP (2006) New Nano technology Research. Nova Publishers 246: 119; Xi N, Chiu Lai KW (2012) Nano-op to electronic Sensors and Devices: Nano photonics from Design to Manufacturing. William Andrew 249: 210.
29. Kane EO (1957) Band structure of indium antimonide. J Phys Chem Solids 1: 249-261.
30. Harutyunyan VA, Kazaryan EM, Sarkisyan HA (2014) Electro absorption in a narrow gap semiconductor nano tube in the field of uniformely charged ring. Physica E 647: 14.
31. Landauand LD, Lifsits EM Course of Theoretical Physics, 3-rded., Quantum Mechanics, non-relativistic Theory 3, (Nauka, Moskow1974, Pergamon, New-York,1977).
32. Handbook of Mathematical Functions, ed. By M Abramovitz and I Steegan (Dover, New-York,1972).
33. TMasselink W, Pearah PJ, Klem J, Peng CK, Morkoc H (1985) Absorption coefficients and excit on oscillator strengths in AlGa As-Ga As super lattices. Physical Review B 32: 8027-8033.
34. Efros AlL, Efros AL (1982) "Inter band absorption of light in a semiconductor sphere". Semiconductors 16: 772-775.
35. Djurišić AB, Li EH, Rakić D, Majewski ML (2000) Modeling the optical properties of AlSb, GaSb, and *InSb*. Applied Physics A 70: 29-32.
36. Van Roosbroeck W, Shockley W (1954) Photon-radiative recombination of electrons and holes in germanium. Physical Review 94: 1558.
37. Bhattacharya R, Pal B, Bansal B (2012) On conversion of luminescence into absorption and the van Roosbroeck-Shockley relation. Applied Physics Letters 100: 222103.
38. Harutyunyan VA, Hayrapetyan DB, Kazaryan EM (2018) Interband Absorption and Photoluminescence in the Cylindrical Layered CdS/HgS/CdS Hetero structure. Journal of Contemporary Physics 53: 48-57.
39. Hayrapetyan DB, Baghdasaryan DA, Kazaryan EM, Pokutnyi SI, Sarkisyan HA (2018) Exciton states and optical absorption in core/shell/shell spherical quantum dot. Chemical Physics 506: 26-30.